

PARTICLE CRUSHING AND DEFORMATION BEHAVIOUR

MAMORU KIKUMOTOⁱ⁾, DAVID MUIR WOODⁱⁱ⁾ and ADRIAN RUSSELLⁱⁱⁱ⁾

ABSTRACT

Particle breakage occurs in granular materials with various engineering applications, such as when driving piles (especially where the strength of the particles is low) and in debris flows (where the energy levels are high), and the influence of this breakage on the mechanical behaviour of soils should be given proper consideration in a constitutive model for soils. Particle breakage results in an increase in the number of fine particles and broadens the grading of particle sizes, and the primary effect of broadening the grading is to lower the critical state line and other characteristics of the volumetric response in the compression plane. In our study, an existing constitutive model, the Severn-Trent sand model, in which the critical state line plays a central role as the locus of asymptotic states, has been extended to include the effects of particle breakage. Severn-Trent sand is a frictional hardening Mohr-Coulomb model described within a kinematic hardening, bounding surface framework. The central assumption is that strength is seen as a variable quantity, dependent on the current value of the state parameter (volumetric distance from the critical state line) which varies with changes in density and stress levels. If the critical state line falls as a result of broadening grading, the state parameter tends to increase and the soil feels looser.

Key words: constitutive equation, (critical states), deformation, elasto-plasticity, grain size distribution, (grading state index), particle breakage, sand, (state parameter), stress-strain relation (**IGC:** D6)

INTRODUCTION

Particle breakage and crushing occur in granular materials during various engineering applications, for example when piles are being driven into sands and in debris flows where the energy levels are rather high. The occurrence of particle crushing implies that the material being tested or being subjected to geotechnical loads is actually changing. The changes are irreversible and uncontrollable so that the material that exists at the end of a pile driving exercise is quite different from the material that was there to begin with, and the properties of the material will also be altered. Results of one-dimensional, high-pressure compression tests on Ottawa quartz sand (Roberts and de Souza, 1958) are shown in Fig. 1 as an example of the effect of particle crushing on the stress:strain response of soils. The sand shows relatively low compressibility initially, but it becomes more compressive at a stress level of around 20–30 MPa (Fig. 1(a)). The sand particles then start to crush significantly and the particle size distribution evolves (Fig. 1(b)). Therefore, the sharp increase in the slope of the compression line at a high stress level appears to be primarily the consequence of fracturing of sand particles.

The grading of a soil will evolve as a result of particle

crushing induced by compression or shearing, and changes in grading will affect the mechanical behaviour of the soil. The material seen once particle breakage has occurred is quite different from the initial material. In this study, we developed a model of soil behaviour which has the ability to take the changing grading into account. Broader gradings enable more efficient packing, so we expect that particle breakage will have a significant effect on asymptotic densities such as the critical states (Schofield and Wroth, 1968; Muir Wood, 1990). Therefore, as the basis for our modelling of crushable soils, we chose a model for uncrushable soils for which the existence of asymptotic critical states plays a central role: Severn-Trent sand (Gajo and Muir Wood, 1999a, b).

SEVERN-TRENT SAND MODEL

Severn-Trent sand (Gajo and Muir Wood, 1999a, b) is an extended Mohr-Coulomb model which brings together four simple relationships, summarised in Fig. 2, in order to describe the typical response of sands of different densities and at different stress levels with a rather modest number of soil parameters.

First, it is proposed that there is a locus of asymptotic, limiting, critical states that the soil seeks when it is

ⁱ⁾ Assistant Professor, Department of Civil Engineering, Nagoya Institute of Technology, Nagoya, Japan (kikumoto@nitech.ac.jp).

ⁱⁱ⁾ Professor, Department of Civil Engineering, University of Dundee, Dundee, Scotland.

ⁱⁱⁱ⁾ Senior Lecturer, School of Civil and Environmental Engineering, University of New South Wales, Sydney, Australia.

The manuscript for this paper was received for review on September 20, 2009; approved on June 8, 2010.

Written discussions on this paper should be submitted before March 1, 2011 to the Japanese Geotechnical Society, 4-38-2, Sengoku, Bunkyo-ku, Tokyo 112-0011, Japan. Upon request the closing date may be extended one month.

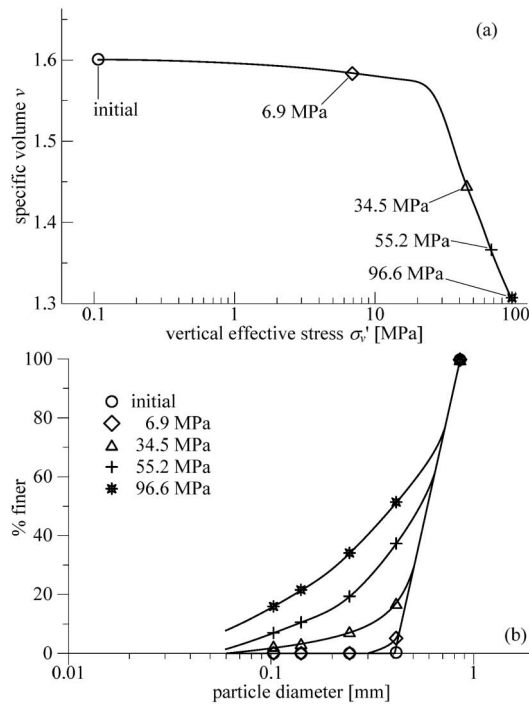


Fig. 1. One-dimensional, high-pressure compression test on Ottawa quartz sand initially uniform particle size (a) compression line in semi-logarithmic $v: \ln \sigma'_v$ plane; (b) evolution of particle size distribution with increase in stress level (after Roberts and de Souza, 1958)

sheared, defined in terms of density or specific volume and a mean effective stress, as indicated in Fig. 2(a). Having identified such a locus, a state parameter ψ (Been and Jefferies, 1985) is defined as the volumetric distance of the current state of the soil from the critical state line at the current mean stress. This state parameter plays a central role in the description of all aspects of the soil response: it seems intuitively reasonable that the soil should have a feeling for the limiting density or packings at its current stress level and adjust its response accordingly.

Second, a typical relationship between the state parameter and strength (Fig. 2(b)) reminds us that the strength of soils should be seen as a dependent rather than an independent quantity. Since the state parameter varies during a test, so also does the current strength.

Third, a monotonic hardening law (Fig. 2(c)) describes the monotonic approach to the current strength with increasing plastic distortional strain. But of course the strength that is sought is not constant because the density or the stress level of the soil changes, and with it the current value of state parameter changes (Fig. 2(b)).

The fourth element of the model is a stress-dilatancy relationship (Fig. 2(d)) which forces volume change towards the critical state whenever distortional straining occurs. There may be dilation or contraction depending on the current value of stress ratio relative to the critical state stress ratio.

Severn-Trent sand is a distortional hardening model which has a purely frictional description of yielding (Fig. 3). As the soil shears plastically, it gradually hardens

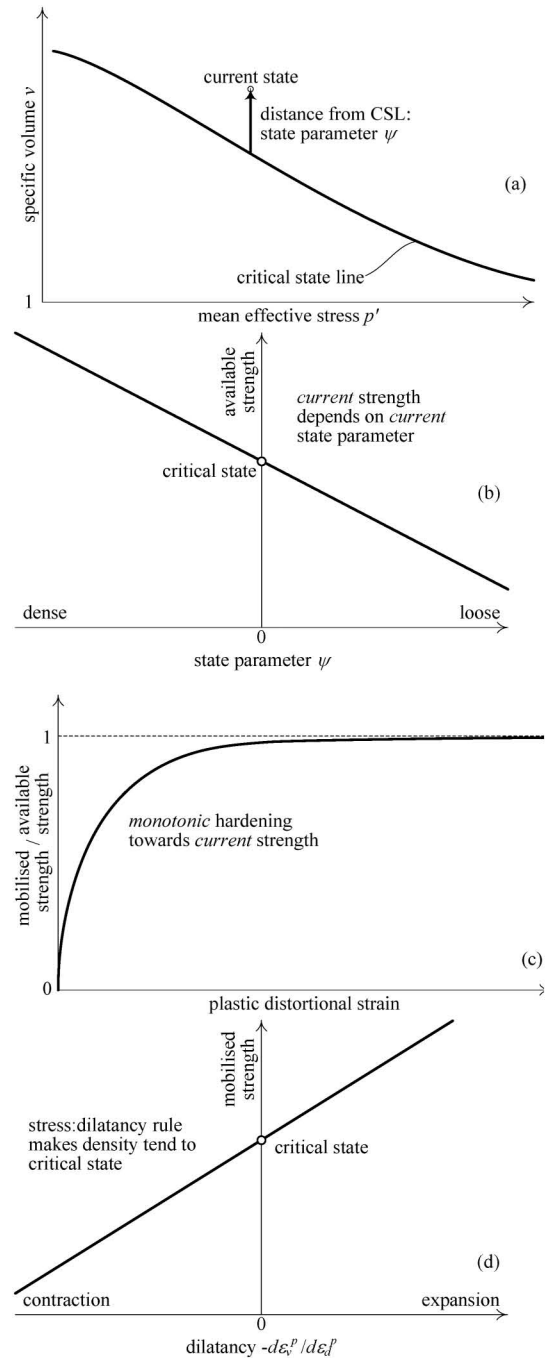


Fig. 2. Severn-Trent sand: (a) critical state line in compression plane and definition of state parameter ψ ; (b) link between current strength and current state parameter; (c) monotonic hardening law; (d) stress:dilatancy relationship

towards the current strength and the sign and the magnitude of the volume changes depend on the mobilised friction and the current value of the state parameter. The effect of this volume change is always to encourage the soil to approach a critical state. The model is able to predict non-monotonic stress-strain response, with a clear peak strength followed by strain softening even though the hardening law is apparently monotonic.

In order to describe non-monotonic loading, a kinematic hardening rule is applied to record the in-

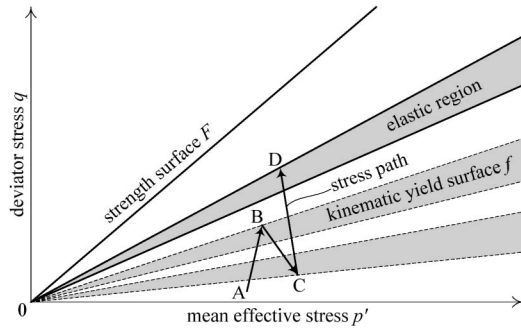


Fig. 3. Severn-Trent sand: frictional yield surface and strength surface in $p':q$ plane

fluence of past stress history on the fabric of the sand (Fig. 3). A small elastic region moves around with the current stress and allows the model to describe the high stiffness that is always associated with deviatoric stress reversal (Alawaji et al., 1990). A bounding surface plasticity framework provides a pragmatic way of describing the steady decrease in shear stiffness from this high elastic stiffness towards an eventual critical state. The model predicts well the stress-strain behaviour of sand of a wide range of densities under both drained and undrained conditions (Gajo and Muir Wood, 1999a, b).

PARTICLE CRUSHING AND ITS CONSTITUTIVE MODELLING

Severn-Trent sand assumes that dilatancy accompanying shearing is the only mechanism by which irrecoverable volumetric strains can occur. Thus, isotropic compression is entirely an elastic process in this model. We now make the assertion that the irrecoverability of volumetric deformation during compression is linked with particle breakage. We retain the Severn-Trent sand model as appropriate to the shearing of sands at stress levels which are low by comparison with the crushing strength of individual particles and proceed to add an extra mechanism to describe the effects of particle breakage and associated change in grading. We propose to tackle this in three stages: first, the selection of a grading index which monitors the changing grading of the soil; second, the generation of an evolution law linking stress and strain history in compression or shearing with change in grading index; and third, the selection of hypotheses to describe the influence of the changing grading on the mechanical response of the soil.

Before taking into account the effect of particle crushing, the critical state line and isotropic compression line for a single, constant grading are defined. Traditionally, the critical state line has been chosen as linear in a semi logarithmic compression plane (that is, the specific volume v versus the logarithm of mean effective stress $\ln p'$). The linear semi logarithmic form is, however, unsatisfactory because it does not recognise physically reasonable limits and it provides a negative void ratio under large stress levels. We know that there must be a low-

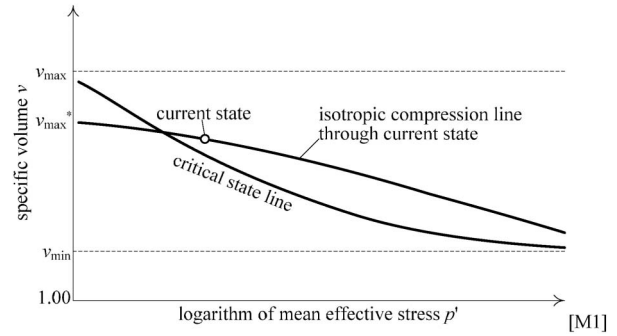


Fig. 4. Critical state line and isotropic compression lines for a single, constant grading

er bound (at least to the specific volume $v = 1$) for very large stresses and we expect that there will be a limiting maximum specific volume at very low stresses. A modified form of the critical state line following Gudehus (1997) is, hence, introduced to the proposed model (Fig. 4).

$$v = v_{\min} + (v_{\max} - v_{\min}) \exp \left[- (p' / p_{cs})^{k_1} \right] \quad (1)$$

where p_{cs} and k_1 are parameters controlling the shape of the critical state line. This equation ensures that the critical state line exists for the range of specific volumes $v_{\max} > v > v_{\min}$. An isotropic, elastic compression line is defined by a similar form.

$$v = v_{\min} + (v_{\max}^* - v_{\min}) \exp \left[- (p' / p_{ic})^{k_1} \right] \quad (2)$$

The current state (specific volume v and mean effective stress p') is always located on this line by adjusting the volumetric variable v_{\max}^* , which is a reference to specific volume at $p' = 0$ satisfying $v_{\max} \geq v_{\max}^* > v_{\min}$. The reference stress p_{ic} ($< p_{cs}$) is a parameter controlling the shape of the isotropic elastic compression line. The elastic bulk modulus K is obtained from Eq. (2):

$$K = \frac{v}{v - v_{\min}} \frac{p_{ic}^{k_1}}{k_1} p'^{1-k_1} \quad (3)$$

and the elastic shear modulus G is also obtained by assuming isotropic elasticity and choosing a constant value for Poisson's ratio v_e . Stress level dependencies of the elastic moduli G and K assumed in the proposed model are broadly similar to those suggested by past researches (Nakai, 1989; Gajo and Muir Wood, 1999a, b).

Grading State Index as a Measure of the Current Changing Grading

Comparisons of evolving gradings as a result of particle crushing (Fig. 5) indicate that the crushing of soil particles occurs as a result of both isotropic compression and shearing, and the major effect of particle crushing is to increase the proportion of fine particles which fill the voids between larger particles without particularly changing the size of the largest particles (e.g., Vesić and Clough, 1968; Coop et al., 2004).

In order to incorporate effects of evolving grading due to particle crushing in a constitutive model, it is con-

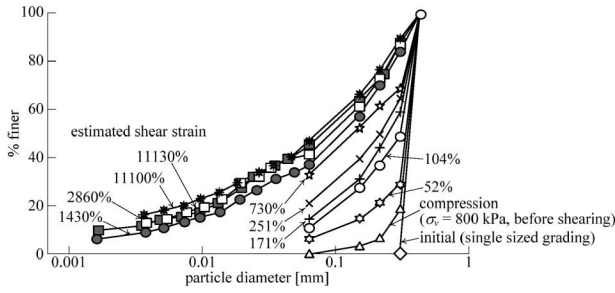


Fig. 5. Evolution of particle size distribution in ring shear tests on Dog's Bay sand (after Coop et al., 2004)

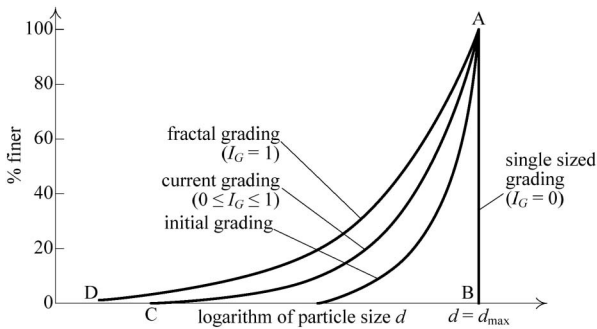


Fig. 6. Schematic diagram of evolving grading and definition of grading state index I_G as ratio of areas ABC and ABD (Muir Wood, 2007)

venient to define a simple index which can indicate where the current varying grading of the soil is located between defined extreme gradings. One natural extreme of particle size distribution is single-sized grading (AB in Fig. 6). The above-mentioned experimental studies (e.g., Fig. 5) indicate that at the other extreme, after a large amount of crushing has occurred due to successive compression or shearing, there is a tendency for the grading to become an increasingly limiting, fractal grading (AC in Fig. 6) where the arrangement of particles looks the same at all scales (McDowell et al., 1996). Although such a fractal limiting grading seems to be physically reasonable, the essential assumption in the proposed model is that there is such a things as limiting grading (this does not have to be fractal) where soil no longer exhibits particle crushing.

The grading state index I_G can, be then, defined as shown in Fig. 6 as the ratio of areas ABC and ABD where area ABD is the area under a limiting particle size distribution (Muir Wood, 2007). The grading state index I_G takes the value 0 at the narrowest, single-sized distribution (AB in Fig. 6) and it takes on the value 1 as grading reaches the limiting distribution (AD in Fig. 6). For sands tested at sufficiently high stress level the particles tend to crush and the grading state index I_G monotonically increases from 0 to 1. Other definitions of the grading state index are obviously possible, but the choice of a parameter with a range 0–1 is useful when modelling the effect of changing grading in a continuum model. The relative breakage B_r defined by Hardin (1985) as the ratio of areas ABC and ABD in Fig. 7 takes a value between 0

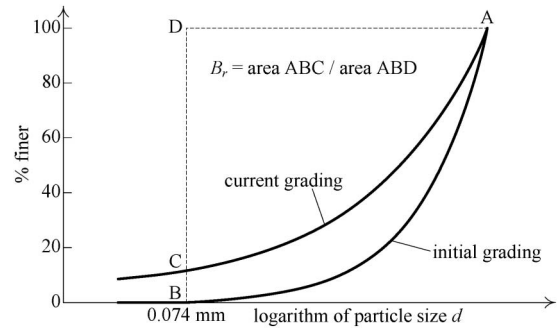


Fig. 7. Definition of breakage parameter B_r as ratio of areas ABC and ABD (after Hardin, 1985)

and 1, which is incrementally proportional to I_G . However, Hardin's scale does not incorporate the idea of fractal grading. There is no experimental support for getting a limiting grading beyond some fractal one so that reaching 1 on the relative breakage B_r is not possible.

Evolution Law of the Grading State Index I_G Due to Particle Crushing

The grading state index I_G bound by 0 for a single-sized grading and 1 for a limiting fractal grading provides a simplified, scalar representation of the current grading. It increases monotonically from 0 to 1 as particle crushing occurs. The grading state index works as an intermediary to describe the evolutions of mechanical properties due to particle crushing. An evolution law is necessary in incorporating the grading state index in order to describe the effects of changing grading in a soil model.

Regarding the onset and evolution of particle crushing, Hardin (1985) proposes a hyperbolic relationship between relative breakage B_r ($\delta B_r \propto \delta I_G$) and breakage stress σ_b based on experimental results:

$$B_r = \frac{\chi^\beta}{1 + \chi^\beta} \quad \text{where} \quad \chi = \frac{\sigma_b}{\sigma_r} \quad (4)$$

β and σ_r are material constants in which the characteristics of soil particles will be reflected ($\sigma_r = 800p_a(\beta - 0.3)$) from empirical study (Hardin, 1984) with p_a equal to atmospheric pressure). The breakage stress σ_b is a variable given as a composite function of mean effective stress p' and deviator stress q :

$$\sigma_b = p' \left[1 + \frac{2\sqrt{2}}{3} \left(\frac{q}{p'} \right)^3 \right] \approx p' [1 + \eta^3] \quad (5)$$

It represents a macroscopic characteristic strength of a granular material and varies with the current stress state. For a given macroscopic mean effective stress p' and material strength σ_r , σ_b increases as the stress ratio η increases, meaning that B_r increases as η increases. Also, for a constant η and σ_r , σ_b and B_r increase as p' increases. Equation (4) implies that the relative breakage B_r will finally reach unity as σ_b tends to infinity. Typical curves linking p' and q for constant relative breakage B_r and variations of B_r with p' (for a constant stress ratio η) are shown in Fig. 8. It is known from this figure that: Eqs.

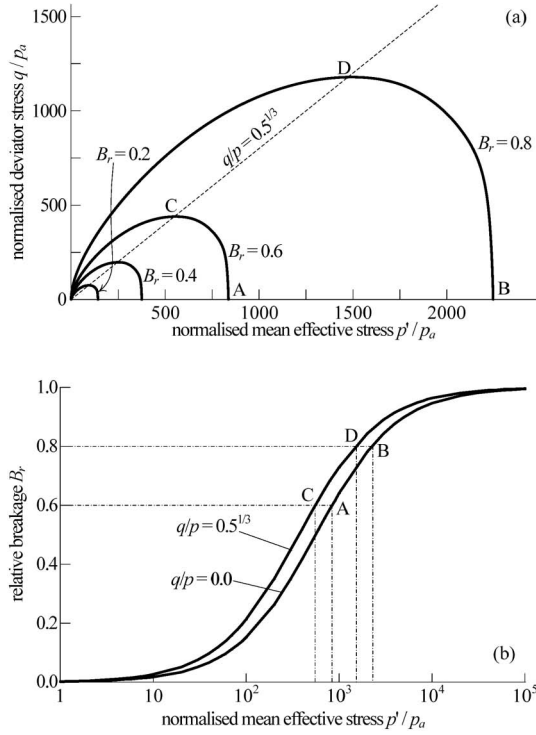


Fig. 8. Relative breakage B_r linked with mean effective stress p' and deviator stress q (a) contours for constant B_r in p' - q plane; (b) increase of B_r with stress level for constant stress ratio q/p

(4) and (5) combine effects of mean stress and mobilised friction on the extent of particle crushing and draw a convex crushing surface in the p : q plane; they provide an evolution law of the extent of grading due to crushing. Russell et al. (2009) derived analogous failure surfaces to those shown in Fig. 8 by considering particle crushing and assembly instability in a theoretical study of stress fields in spherical particles belonging to idealized uniform granular assemblies. Other researchers (e.g., Coop and Lee, 1993) have also mentioned that the extent of particle crushing has a close relationship with stresses. The experimental results shown in Fig. 9 indicate that the relative breakage B_r has a unique relationship with mean effective stress p' for constant stress ratio ($\eta = 0$, M where M is critical state strength).

From the above discussions, the simplest way to describe the evolution of the grading state index I_G seems to be to link crushing with stress histories. This has the advantage that if the stresses stop changing then the particle crushing will also stop even if shearing continues. Although it is an attract concept to link the grading evolution to plastic strain or plastic work, it predicts the continued evolution of grading to a limiting one at the critical state regardless of stress level. While the grading state index I_G was applied instead of relative breakage in this study, a similar crushing criterion ($f_c = 0$ in Fig. 10) and its hardening rule (Fig. 11) can be introduced as a second yield mechanism. Figure 10 simply shows the triaxial section to illustrate the general principles, using the mean effective stress and deviator stress in the usual way. It is assumed for convenience that: particle crushing occurs

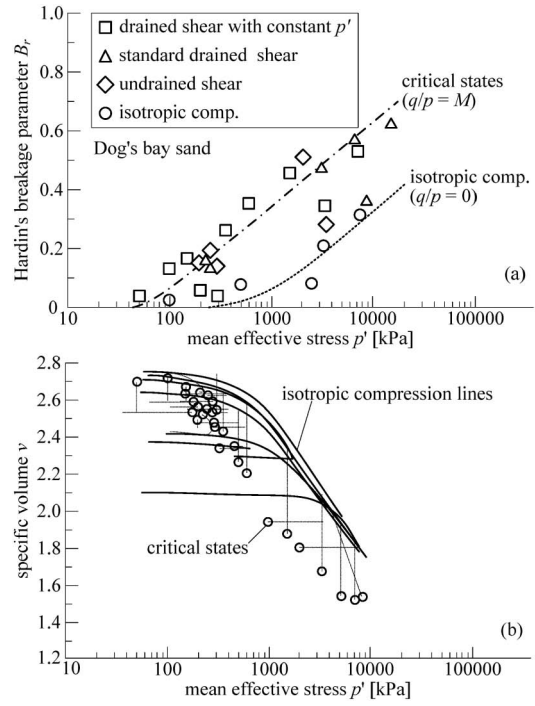


Fig. 9. Results of isotropic compression, drained and undrained triaxial compression tests on Dog's Bay sand (a) extent of particle crushing due to isotropic compression and shear; (b) isotropic compression lines and critical state line in compression plane (after Coop and Lee, 1993)

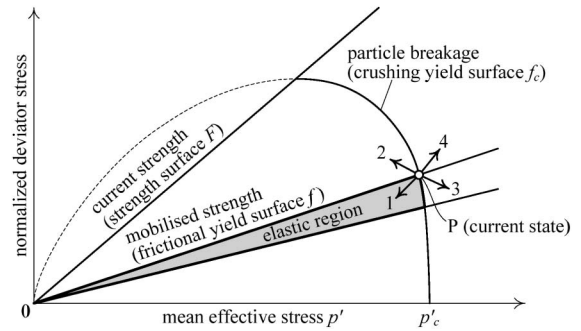


Fig. 10. Strength locus, distortional yield locus and crushing yield locus in normalised stress plane

when the current stress state intersects the crushing surface ($f_c = 0$ and $df_c > 0$); the size p_c of crushing surface representing the maximum stress level in the past history (pre-compression stress) is selected as the hardening parameter so that only hardening occurs ($dp'_c \geq 0$); plastic strains for this mechanism obey a simple associated flow rule. The yield loci are scaled in such a way that the normal is vertical (implying purely distortional response) where they cross the strength line, as shown in Fig. 10. Meanwhile the plastic strains for the distortional mechanism follow a non-associated flow rule as the original Severn-Trent sand as hinted in Fig. 2(d). Because the frictional strength of the soil is a variable dependent on the current value of state parameter ψ , it is convenient to formulate much of the theoretical development of the model

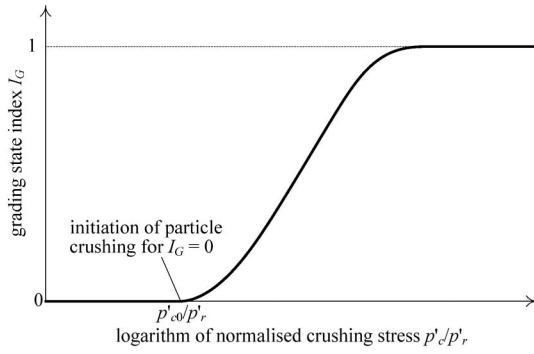


Fig. 11. Variation of crushing stress p'_c with I_G

in a normalised stress space. If strength is dependent on state parameter according to a linear relationship: $\eta_p = M(1 - k\psi)$ where k is a soil parameter, then, instead of considering variability of strength, we can normalise deviator stresses by dividing by $(1 - k\psi)$ and correspondingly introduce a normalised stress ratio $\bar{\eta} = \bar{q}/p' = q/[p'(1 - k\psi)]$. The second yield mechanism which describes the onset of particle crushing is thus given as a function of normalized stress:

$$f_c = p' \left[1 + \frac{1}{2} \left(\frac{\bar{\eta}}{M} \right)^3 \right] - p_c = 0 \quad (6)$$

which has broad similarities to Eq. (5), now with the size p_c of the crushing surface representing a macroscopic characteristic strength.

The hardening parameter p_c is linked with the current grading expressed through the grading state index I_G :

$$I_G = 1 - \exp \left[- \left(\frac{p_c - p_{c0}}{p_r} \right)^{k_2} \right] \quad (7)$$

where p_{c0} is the size of the crushing surface for $I_G = 0$ (single-sized grading), describing the initiation of particle crushing; k_2 is a soil parameter and p_r is a reference stress (Fig. 11). Equations (6) and (7) ensure that I_G monotonically increases from 0 to 1 with the increase of p_c to infinity. The crushing behaviour of soil particles obviously depends on properties of individual grains (such as mineralogy, hardness, shape and size) and environmental conditions (such as packing density, particle size distribution, stress level and mobilised friction), which would be reflected in the soil parameters k_2 , p_r and p_{c0} .

Influence of the Increasing Grading State Index on Mechanical Behaviour

The grading state index I_G and its evolution law allow us to predict how soil grading evolves as a result of particle crushing. Laws describing how the change in I_G affects the mechanical properties of soils are, then, needed in order to describe the effect of particle crushing in a constitutive model. Several experimental studies (e.g., Roberts and de Souza, 1958; Coop and Lee, 1993) indicate that the crushing and fracturing of particles increases the compressibility of sands, which is already illustrated in Fig. 1. Miura and O-Hara (1979) mention that particle

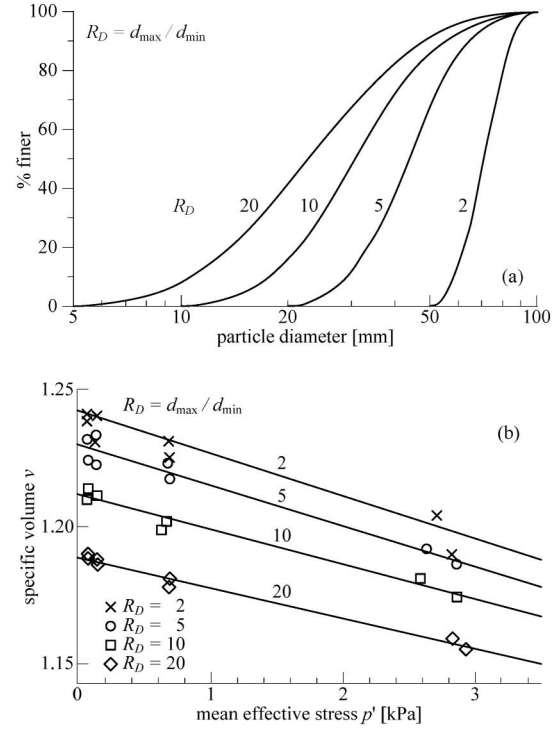


Fig. 12. Effects of grading on stress:strain relation and critical state line: biaxial tests using various gradings of circular discs for 2-d DEM analysis (a) particle size distributions; (b) critical state lines in compression plane (after Muir Wood and Maeda, 2007)

crushing increases the negative dilatancy, which may reduce the peak shear strength. Hyodo et al. (1998) note that crushable soils, when sheared in a dense state, trace undrained stress paths similar to those for loose sands of a less crushable nature. Mahboubi et al. (1997) suggest that soil samples of different initial densities tend to the same void ratio owing to shearing but this void ratio continues to fall as breakage continues. These aspects of soil behaviour need to be described by linking the evolving grading state index I_G with the stress:strain characteristics of soil.

Past experimental studies (Coop, 1990; Coop et al., 2004; Russell and Khalili, 2004) have indicated that the mobilised friction angle at residual state does not considerably change regardless of significant amount of particle crushing whereas the peak friction angle depends on the density and stress level. Therefore, to first order, the friction angle at critical state is assumed to be constant in the proposed model because the mineralogy of the crushing particles does not undergo any change.

Although there are not many studies into the effect of particle crushing on the stress:dilatancy relationship, it is indicated through the discrete element analysis by Muir Wood and Maeda (2007) that the stress:strain relations of samples of different gradings are very similar to each other provided that the relative density is the same (Fig. 12) and that grading, consequently, has little influence on stress:dilatancy relationship. A first order assumption in the proposed model would, therefore, be to assume that the stress:dilatancy relationship is uniquely determined

regardless of the current state of grading.

However, it seems reasonable to propose that, as the soil particles crush and efficiently fill the voids, the reference packings of the soil becomes denser, the maximum and minimum specific volumes correspondingly fall, and any soil property linked with the reference packings including the specific volume at critical state or isotropic compression state is affected. Experimental results on artificial mixtures of soil particles of different sizes (Zlatović and Ishihara, 1995; Lade et al., 1998; Coop et al., 2004) indicate how the addition of fine particles affects the reference specific volumes such as maximum, minimum and critical state specific volume of a stable material. Initially, the finer particles are able to distribute themselves freely within the voids of the coarser particles and the reference void ratios fall. If more and more fine material is added artificially then eventually the finer particles start to push apart the larger particles and the void ratios rise again. However, this is a mode of behaviour only observed so far within an artificial mixture. Critical states approached by a crushing soil over a wide range of confining pressure are shown in Fig. 9 (Coop and Lee, 1993; Vesić and Clough, 1968). Although some researchers have modeled such a curved critical state zone involving the effect of crushing by two or three-part critical state lines (for example, Russell and Khalili, 2002), the grading state index rises during particle crushing and the material changes. This is, hence, not a critical state line for a single, constant grading. The evolution of a critical state line for a soil exhibiting particle crushing and its non-uniqueness are observed in an experimental study on crushable Okinawa sand (Tojo et al., 2009) (Fig. 13) and discrete element analysis of assemblies of agglomerates (Cheng et al., 2005). It is suggested from Figs. 9, 12(b) and 13 that critical state lines move downward in the compression plane of mean stress p' and specific volume v (specific volume v at critical state is reduced) as the soil grading becomes broader as a result of particle crushing while its slope or shape does not change very much.

Constitutive models such as Severn-Trent sand which include a critical state line as a basic feature controlling strength and dilatancy as a function of state parameter will be particularly affected by the possibility of changing position of the critical state line, but incorporation of such influences of particle crushing can be achieved relatively simply by linking the position of the critical state line in the compression plane to the grading state index I_G . By considering the grading state index as an extra dimension of critical states, the critical state line in the compression plane of specific volume v and mean stress p' , then, becomes a three dimensional critical state surface of specific volume v , mean stress p' and grading state index I_G , such as that shown in Fig. 14. In the proposed model, we assume that the values of v_{\max} and v_{\min} in Eq. (1) are dependent on the grading state index I_G . For single sized grading, for which the grading state index I_G is zero, the minimum specific volume for a packing of spheres is theoretically proved to be $\sqrt{18}/\pi \cong 1.35$ (the Kepler conjecture) (Hales, 2005). In another idealised case, a pack-

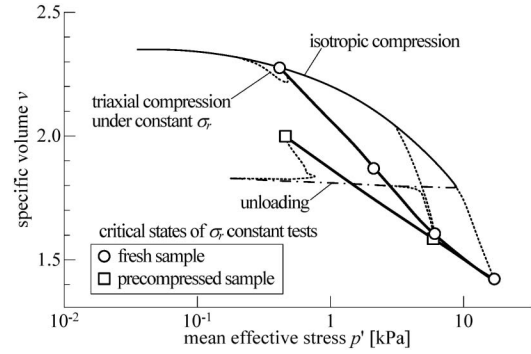


Fig. 13. End points of shearing tests: effect of precompression on critical states observed in drained conventional triaxial compression tests on crushable Okinawa sand (after Tojo et al., 2009)

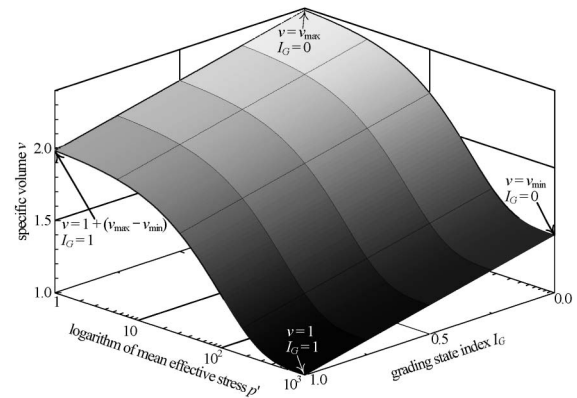


Fig. 14. Critical state surface of mean stress p' , specific volume v and grading state index I_G

ing of limiting grading ($I_G=1$) would be able to be as efficient as the Apollonian fractal packing (e.g., Kasner and Supnick, 1943) for which the specific volume is equal to unity because successively finer particles occupy the void spaces between their coarser neighbours. Thus, as the grading changes from a single sized one to a limiting fractal one and the grading state index I_G increases from 0 to 1, we assume that the minimum specific volume decreases from v_{\min}^i to 1 and the maximum specific volume decreases from v_{\max}^i by the same amount $v_c (=v_{\min}^i - 1)$ as v_{\min} .

$$v_{\min} = v_{\min}^i - v_c I_G \quad (8)$$

$$v_{\max} = v_{\max}^i - v_c I_G \quad (9)$$

where v_{\min}^i and v_{\max}^i are constitutive parameters determining the minimum and maximum specific volumes for the single sized grading ($I_G=0$). By substituting Eqs. (8) and (9) into Eq. (1), the critical state surface considering the evolution of grading is given as a function of specific volume v , mean stress p' and grading state index I_G .

$$v = v_{\min}^i - v_c I_G + (v_{\max}^i - v_{\min}^i) \exp[-(p'/p_{cs})^{k_1}] \quad (10)$$

Equation (10) defines a three dimensional critical state surface in $p':v:I_G$ space (Fig. 14). The non-uniqueness of a critical state line in the $v:\ln p'$ compression plane such as shown in Figs. 12(d) and 13 is simply a projection onto

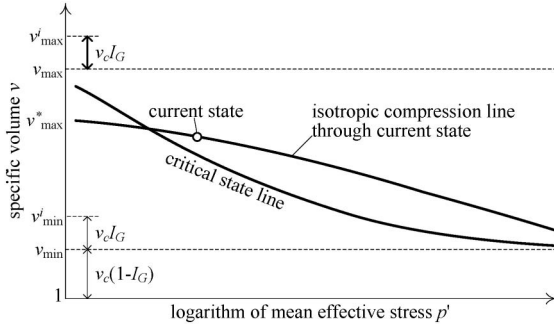


Fig. 15. Critical state line and isotropic compression line for a certain value of the grading index I_G

this plane of a section through the three dimensional surface.

As reference specific volumes decrease due to the increase in I_G , the isotropic compression line also moves downward in the compression plane. By substituting Eqs. (8) and (9) into Eq. (2), we can obtain a three dimensional isotropic compression surface in $p':v:I_G$ space of the form:

$$v = v_{\min}^i - v_c I_G + [v_{\max}^* - (v_{\min}^i - v_c I_G)] \exp \left[- (p'/p_{ic})^{k_1} \right] \quad (11)$$

Critical state line and isotropic compression line for a certain value of the grading index I_G , which is drawn in the $v:p'$ plane by Eqs. (10) and (11), are shown in Fig. 15. In order to ensure that particle crushing always leads to volumetric compression and makes soil feel looser, variation in the specific volume owing to the particle crushing mechanism (δv^c) is given by a scaled amount dependent on v_{\max}^* :

$$\delta v^c = -K_c v_c \delta I_G = - \frac{v_{\max}^* - v_{\min}^i}{v_{\max}^i - v_{\min}^i} v_c \delta I_G \quad (12)$$

which then implies that the total volumetric strain linked with the crushing yield mechanism (which is non-reversible and therefore purely plastic) is:

$$\delta \varepsilon_p^c = \delta \varepsilon_p^{pc} = \frac{K_c v_c \delta I_G}{v} \quad (13)$$

The scaled amount K_c defined in Eq. (12) is a variable with a range 0–1 controlling the amount of plastic volumetric compression due to particle crushing, which ensures that the current specific volume v of crushing soil never becomes less than the minimum specific volume v_{\min}^i for the current grading. Evolutions of critical state line and isotropic compression line due to the increase in the grading state index are schematically shown in Fig. 16.

State Parameter and Normalised Stress Tensor Considering the Effect of Changing Grading

The state parameter ψ , which controls the current available (peak) strength of the sand, represents the volumetric distance of the current state of the soil from the critical state line at the current mean stress and the current grading state index (Fig. 17). The state parameter in

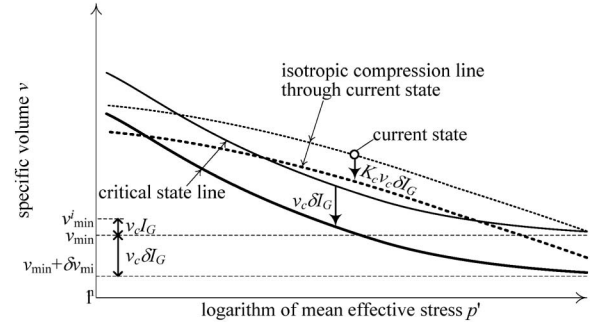


Fig. 16. Critical state line and isotropic compression lines fall as I_G increases

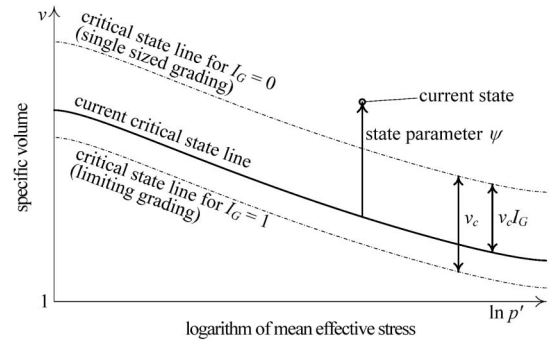


Fig. 17. State parameter ψ as a volumetric distance of the current state from critical state at the current mean stress and the current grading state index

which the influence of changing grading is considered is, thus, given from Eq. (10).

$$\psi = v - v_{cs} = v - v_{\min}^i + v_c I_G - (v_{\max}^i - v_{\min}^i) \times \exp \left[- (p'/p_{cs})^{k_1} \right] \quad (14)$$

Stress tensor normalised using the state parameter and their invariants are given in the same way as the original Severn-Trent sand

$$\bar{\sigma}_{ij} = \frac{s_{ij}}{1 - k\psi} + p\delta_{ij} \quad (15)$$

where s_{ij} is the deviator stress tensor. Variation in the state parameter ψ becomes:

$$\delta \psi = \frac{\partial \psi}{\partial \varepsilon_{ij}} \delta \varepsilon_{ij} + \frac{\partial \psi}{\partial \sigma_{ij}} \delta \sigma_{ij} + \frac{\partial \psi}{\partial I_G} \delta I_G$$

where

$$\begin{cases} \frac{\partial \psi}{\partial \varepsilon_{ij}} = -v\delta_{ij} \\ \frac{\partial \psi}{\partial \sigma_{ij}} = (v_{\max}^i - v_{\min}^i) \frac{k_1}{p} \left(\frac{p}{p_{cs}} \right)^{k_1} \exp \left[- \left(\frac{p}{p_{cs}} \right)^{k_1} \right] \frac{\delta_{ij}}{3} \\ \frac{\partial \psi}{\partial I_G} = v_c \end{cases} \quad (16)$$

where δ_{ij} is Kronecker's delta. The state parameter increases as the grading index I_G increases during crushing, the current peak strength falls and therefore particle

crushing makes the soil feel looser as a consequence. From Eq. (7) an increment of the grading state index I_G is linked with the increase in the size p_c of the crushing surface.

$$\delta I_G = \frac{\partial I_G}{\partial p_c} \delta p_c$$

where

$$\frac{\partial I_G}{\partial p_c} = \frac{k_2(p_c - p_{c0})^{k_2-1}}{p_r^{k_2}} \exp \left\{ - \left(\frac{p_c - p_{c0}}{p_r} \right)^{k_2} \right\} \quad (17)$$

An increment of the size of the particle crushing surface p_c is linked with the increment of the normalised stress tensor by Eq. (6).

$$\delta p_c = \frac{\partial f_c}{\partial \bar{\sigma}_{ij}} \delta \bar{\sigma}_{ij} = \left(\frac{\partial f_c}{\partial p} \frac{\partial p}{\partial \bar{\sigma}_{ij}} + \frac{\partial f_c}{\partial \bar{q}} \frac{\partial \bar{q}}{\partial \bar{\sigma}_{ij}} \right) \delta \bar{\sigma}_{ij}$$

where

$$\begin{cases} \frac{\partial f_c}{\partial p} \frac{\partial p}{\partial \bar{\sigma}_{ij}} = \left\{ 1 - \left(\frac{\bar{\eta}}{M} \right)^3 \right\} \frac{\delta_{ij}}{3} \\ \frac{\partial f_c}{\partial \bar{q}} \frac{\partial \bar{q}}{\partial \bar{\sigma}_{ij}} = \frac{3\bar{\eta}^2}{2M^3} \left(\sqrt{\frac{3}{2s_{kl}s_{kl}}} s_{ij} \right) \end{cases} \quad (18)$$

CONSTITUTIVE RELATIONS AND STIFFNESS TENSORS

Four Possibilities of Loading Conditions

In Fig. 10, there are four possibilities of loading conditions which need to be considered in numerical implementation for a given stress state P , which sits on both the distortional yield locus and the particle crushing yield locus: 1 ($f < 0 \vee df < 0$) \wedge ($f_c < 0 \vee df_c < 0$): the stress is unloading for both mechanisms and purely elastic response is predicted; 2 ($f = 0 \wedge df \geq 0$) \wedge ($f_c < 0 \vee df_c < 0$): only the distortional mechanism is engaged; 3 ($f < 0 \vee df < 0$) \wedge ($f_c = 0 \wedge df_c \geq 0$): only the particle crushing mechanism is engaged; 4 ($f = 0 \wedge df \geq 0$) \wedge ($f_c = 0 \wedge df_c \geq 0$): both mechanisms are engaged. Procedures for calculating the stiffness tensors for the loading conditions 1 and 2 are the same as those in the original Severn-Trent sand (Gajo and Muir Wood, 1999a, b), and the stiffness tensor for the loading condition 3 is provided in the same way as usual elasto-plastic models using Eq. (6) and assuming the associated flow rule for the particle crushing mechanism. Thus, the elasto-plastic constitutive relation in the case of the loading condition 4 is mainly explained here.

Elastic Constitutive Relations

The elastic constitutive relation is given between the ordinary effective stress increments $\delta \sigma_{ij}$ and the elastic strain increments $\delta \varepsilon_{ij}^e$ as

$$\delta \sigma_{ij} = D_{ijkl}^e \delta \varepsilon_{kl}^e \quad (19)$$

where assuming usual isotropic elasticity,

$$D_{ijkl}^e = \frac{3(1-\nu_e)K}{1+\nu_e} \delta_{ik} \delta_{jl} + \frac{3\nu_e K}{1+\nu_e} \delta_{ij} \delta_{kl} \quad (20)$$

and K are the elastic bulk modulus given by Eq. (3) and ν_e is Poisson's ratio.

Substituting Eqs. (17) and (18) into Eq. (16), the increment in the state parameter can be expressed by stress and strain increments.

$$\delta \psi = \frac{\partial \psi}{\partial \varepsilon_{ij}} \delta \varepsilon_{ij} + \frac{\partial \psi}{\partial \sigma_{ij}} \delta \sigma_{ij} \quad (21)$$

Differentiating Eq. (15), the elastic relation in a normalised stress space becomes

$$\begin{aligned} \delta \bar{\sigma}_{ij} &= \delta p \delta_{ij} + \frac{\delta s_{ij}}{(1-k\psi)} + \frac{ks_{ij} \delta \psi}{(1-k\psi)^2} \\ &= \left[\left\{ \frac{\delta_{ik} \delta_{jl}}{(1-k\psi)} - \frac{k\psi \delta_{ij} \delta_{kl}}{3(1-k\psi)} + \frac{ks_{ij}}{(1-k\psi)^2} \frac{\partial \psi}{\partial \sigma_{kl}} \right\} D_{klmn}^e \right. \\ &\quad \left. + \frac{ks_{ij}}{(1-k\psi)^2} \frac{\partial \psi}{\partial \varepsilon_{mn}} \right] \delta \varepsilon_{mn}^e + \left[\frac{ks_{ij}}{(1-k\psi)^2} \frac{\partial \psi}{\partial \varepsilon_{kl}} \right] \delta \varepsilon_{kl}^p \\ &= \bar{D}_{ijkl}^e \delta \varepsilon_{kl}^e + A_{ijkl} \delta \varepsilon_{kl}^p \end{aligned} \quad (22)$$

where \bar{D}_{ijkl}^e is the equivalent elastic stiffness tensor.

Elasto-plastic Constitutive Relations

Total strain increment is given as summation of elastic and plastic strain increments. For loading condition 4 for which both the distortional mechanism and the particle crushing mechanism are engaged in a same way as Koiter (1953), plastic strain increments consist of each component

$$\delta \varepsilon_{ij} = \delta \varepsilon_{ij}^e + \delta \varepsilon_{ij}^p = \delta \varepsilon_{ij}^e + \delta \varepsilon_{ij}^{pd} + \delta \varepsilon_{ij}^{pc} \quad (23)$$

where elastic strain increment is given from Eq. (22)

$$\delta \varepsilon_{ij}^e = \bar{D}_{ijkl}^{e-1} (\delta \bar{\sigma}_{kl} - A_{klmn} \delta \varepsilon_{mn}^p) \quad (24)$$

and plastic strain increment is

$$\delta \varepsilon_{ij}^p = \left(\frac{m_{ij} n_{kl}}{H} + \frac{m_{ij}^c n_{kl}^c}{H^c} \right) \delta \bar{\sigma}_{kl} \quad (25)$$

where m_{ij} represents the direction of plastic strain increment for the distortional mechanism, n_{ij} is a unit direction tensor normal to the distortional yield surface in the normalised stress space, and H is a plastic coefficient for this mechanism. By assuming an associated flow rule for the particle crushing mechanism, the second order tensor m_{ij}^c representing the direction of plastic strain increment due to particle crushing is given from Eq. (6).

$$m_{ij}^c = \frac{\partial f_c}{\partial \sigma_{ij}} = \frac{\partial f_c}{\partial p} \frac{\partial p}{\partial \sigma_{ij}} + \frac{\partial f_c}{\partial \bar{q}} \frac{\partial \bar{q}}{\partial \sigma_{ij}}$$

where

$$\begin{cases} \frac{\partial p}{\partial \sigma_{ij}} = \frac{1}{3} \delta_{ij} \\ \frac{\partial \bar{q}}{\partial \sigma_{ij}} = \frac{s_{ij}}{1-k\psi} \sqrt{\frac{3}{2s_{kl}s_{kl}}} \end{cases} \quad (26)$$

n_{kl}^c and H^c in Eq. (25) is obtained by Eq. (13).

$$\frac{n_{ij}^e}{H^c} = \frac{K_c v_c}{v m_{ij}^e} \frac{\partial I_G}{\partial p_c} \frac{\partial p_c}{\partial \bar{\sigma}_{ij}} \quad (27)$$

Substituting Eqs. (24) to (27) into Eq. (23), the elasto-plastic stress-strain relation in the normalised stress space is given

$$\delta \bar{\sigma}_{ij} = \bar{D}_{ijkl}^e \delta \varepsilon_{kl} - \bar{D}_{ijkl}^e \frac{m_{kl}^*}{H} \delta f_{\bar{\sigma}} - \bar{D}_{ijkl}^e \frac{m_{kl}^{c*}}{H_c} \delta f_{c\bar{\sigma}}$$

where

$$\begin{cases} m_{ij}^* = m_{ij} + \bar{D}_{ijkl}^{-1} A_{klmn} m_{mn} \\ m_{ij}^{c*} = m_{ij}^e + \bar{D}_{ijkl}^{-1} A_{klmn} m_{mn}^c \\ \delta f_{\bar{\sigma}} = n_{ij} \delta \bar{\sigma}_{ij} \\ \delta f_{c\bar{\sigma}} = n_{ij}^e \delta \bar{\sigma}_{ij} \end{cases} \quad (28)$$

Arranging Eq. (28), we obtain

$$\begin{aligned} n_{ij} \bar{D}_{ijkl}^e \delta \varepsilon_{kl} &= P \delta f_{\bar{\sigma}} + P_c \delta f_{c\bar{\sigma}} \\ n_{ij}^e \bar{D}_{ijkl}^e \delta \varepsilon_{kl} &= Q \delta f_{\bar{\sigma}} + Q_c \delta f_{c\bar{\sigma}} \end{aligned}$$

where

$$\begin{cases} P = 1 + n_{ij} \bar{D}_{ijkl}^e \frac{m_{kl}^*}{H}, & P_c = n_{ij} \bar{D}_{ijkl}^e \frac{m_{kl}^{c*}}{H_c} \\ Q = n_{ij}^e \bar{D}_{ijkl}^e \frac{m_{kl}^*}{H}, & Q_c = 1 + n_{ij}^e \bar{D}_{ijkl}^e \frac{m_{kl}^{c*}}{H_c} \end{cases} \quad (29)$$

From Eq. (29), the following equations are given.

$$\begin{aligned} \delta f_{\bar{\sigma}} &= B_{ij} \bar{D}_{ijkl}^e \delta \varepsilon_{kl} \\ \delta f_{c\bar{\sigma}} &= C_{ij} \bar{D}_{ijkl}^e \delta \varepsilon_{kl} \end{aligned}$$

where

$$\begin{cases} B_{ij} = \frac{Q_c n_{ij} - P_c n_{ij}^e}{P Q_c - P_c Q} \\ C_{ij} = \frac{P n_{ij}^e - Q n_{ij}}{P Q_c - P_c Q} \end{cases} \quad (30)$$

Finally, the elasto-plastic stress-strain relation in the normalised stress space is given

$$\begin{aligned} \delta \bar{\sigma}_{ij} &= \left\{ \bar{D}_{ijkl}^e - \bar{D}_{ijmn}^e \left(\frac{m_{mn}^*}{H} B_{op} + \frac{m_{mn}^{c*}}{H_c} C_{op} \right) \bar{D}_{opkl}^e \right\} \delta \varepsilon_{kl} \\ &= \bar{D}_{ijkl}^{ep} \delta \varepsilon_{kl} \end{aligned} \quad (31)$$

This relation is then converted into the elasto-plastic constitutive relation in ordinary stress space

$$\begin{aligned} \delta \sigma_{ij} &= \delta \bar{p} \delta_{ij} + (1 - k\psi) \delta \bar{s}_{ij} - k \bar{s}_{ij} \delta \psi \\ &= \left[\left\{ (1 - k\psi) \delta_{ik} \delta_{jl} + \frac{k\psi}{3} \delta_{ij} \delta_{kl} - k \bar{s}_{ij} \frac{\partial \psi^*}{\partial \bar{\sigma}_{kl}} \right\} \right. \\ &\quad \left. \times \bar{D}_{kijmn}^{ep} - k \bar{s}_{ij} \frac{\partial \psi}{\partial \varepsilon_{mn}} \right] \delta \varepsilon_{mn} \\ &= D_{ijkl}^{ep} \delta \varepsilon_{kl} \end{aligned} \quad (32)$$

SIMULATIONS

In the present paper, in order to discuss the performance of the proposed model considering the effects of particle crushing, model simulations are compared with those given by the original Severn-Trent sand model assuming a unique critical state line in the compression plane. As the original model describes the response of soil of a constant grading, influences of particle crushing on the stress-strain behaviour can be grasped through the comparisons of these two models.

Throughout this section, the analyses have been carried out using the same set of constitutive parameters for Severn-Trent sand listed in Table 1. Soil parameters v_{\max}^i , v_{\min}^i , p_{cs} , p_{ic} and k_1 , by which the critical state line and isotropic compression line in $v:p'$ plane are described, are determined by the results of undrained triaxial compression tests on Hostun sand RF summarised by Gajo and Muir Wood (1999b). The assumed position of the critical state line is shown in Fig. 18 with critical state specific

Table 1. Constitutive parameters of Severn-Trent sand

parameter	value	description
v_{\max}^i	2.40	maximum specific volume for $I_G = 0$ (uniform particle size)
v_{\min}^i	1.40	minimum specific volume for $I_G = 0$ (uniform particle size)
p_{cs}/p_a	5.0	normalised reference stress for critical state line
p_{ic}/p_a	5.0×10^5	normalised reference stress for isotropic compression line
k_1	0.1	exponent of critical state line and isotropic compression line
ϕ	31.0	critical state angle of friction
ν	0.2	Poisson's ratio
R	0.1	ratio of sizes of yield surface and strength surface
B	0.0016	parameter controlling hyperbolic stiffness relationship
k	2.0	link between changes in state parameter and current strength
A	0.9	multiplier in flow rule

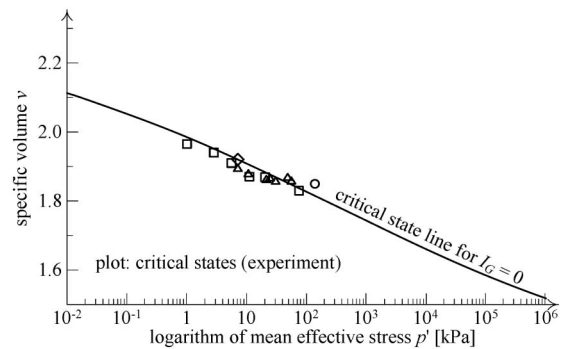


Fig. 18. Critical states observed in undrained triaxial tests and assumed critical state line

Table 2. Constitutive parameters for the particle crushing mechanism

parameter	value	description
p_{c0}/p_a	5.0	normalised size of the crushing surface for $I_G = 0$
p_r/p_a	50.0	normalised reference stress for evolution of I_G
k_2	0.9	exponent of evolution rule of I_G

volumes observed in the past experiments. The critical state friction angle ϕ_{cv} of Hostun sand RF, which is usually measured in triaxial tests by many researchers (e.g., Konrad et al., 1991), is determined to be 31 degrees in the present study. The remaining parameters in Table 1, whose values are deduced through a trial and error procedure and also a global optimization procedure based on the Simplex method, are same as those of Hostun sand RF listed in the papers by Gajo and Muir Wood (1999a, b).

For the particle crushing mechanism, constitutive parameters p_{c0} , p_r and k_2 for the evolution law of the grading state index I_G due to the stress histories are needed. Although their values can be determined by checking the variations in the particle size distribution during isotropic or one-dimensional compression, values listed in Table 2 are determined arbitrarily in the present study so that the grading index starts increasing from a relatively small stress level compared with the actual Hostun sand RF and the influences of particle crushing on the mechanical response will be clearly examined. Note that the response of the proposed model would be identical to that of the original model provided so that the grading state index is kept constant.

To maintain simplicity, the initial position of the axis of the distortional, kinematic yield surface is assumed to coincide with the hydrostatic axis (space diagonal) and the initial anisotropy is thus neglected. The initial value of the grading state index I_G is assumed to be zero so that the assumed initial grading is single sized grading.

Simulations of Isotropic Compression Tests

A series of isotropic compression tests have been performed with varying initial densities (or specific volumes) (Fig. 19). In the simulations by the original Severn-Trent sand in which the effect of particle crushing is not taken into account, only elastic volumetric compression is exhibited and compressibility of sands is rather low (dotted lines in Fig. 19(a)). On the other hand, it is indicated through the simulations by the proposed model considering particle crushing that: the grading index I_G starts to rise once the stress state reaches the particle crushing surface f_c (where mean effective stress $p = p_{c0}$) (Fig. 19(b)), and the volumetric compression of sands become remarkable after this (solid lines in Fig. 19(a)); the amount of compression in a loose state is larger than that in a dense state; the grading state index nearly converges to unity, and particle crushing becomes negligible at around 30–50 MPa (Fig. 19(b)) so that the compressibility of sands is decreased again. These results are consistent with the ob-

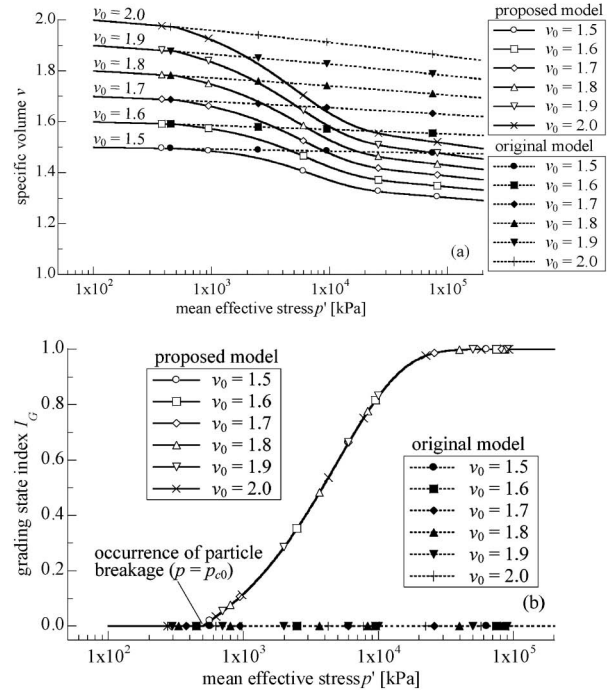


Fig. 19. Simulations of isotropic compression tests of samples with different initial densities: (a) variations of specific volume v ; (b) evolution of grading state index I_G

served behaviour of actual crushing soil, as shown in Fig. 1 (Roberts and de Souza, 1958).

As is seen in Fig. 19(b), the variations in I_G of the samples of different initial densities are identical provided that the effective stress paths are same, which is contradictory to results showing granular materials in a looser state start exhibiting particle crushing under a smaller stress level than denser ones (e.g., Bopp and Lade, 2005; Russell et al., 2009). This is because the evolution rule of I_G is merely related to the stress histories in this model, but such a phenomena can be considered by extending the evolution rule of I_G to be able to consider the influence of the packing density. Some researchers also mention that cyclic loading encourages continuous particle crushing (Hyodo et al., 2002; Coop et al., 2004). Though such a phenomenon is not considered in this model for the sake of simplicity, this could be considered by introducing the concept of a subloading surface (Hashiguchi, 1980) or a bounding surface (Dafalias, 1986) to the particle crushing surface.

Simulations of Drained Triaxial Compression Tests

Three series of simulations of drained shearing tests have been performed here. First, examples of a stress:strain relationships along a drained shearing path under a constant mean effective stress ($p' = 100$ kPa) for dense sample ($v_0 = 1.60$) and loose sample ($v_0 = 1.90$) are shown in Figs. 20 and 21. Although these results are obtained using the proposed model considering the effect of particle crushing, the effective stress path given in the simulation is a shearing path within the crushing surface and the results are identical to those obtained by the origi-

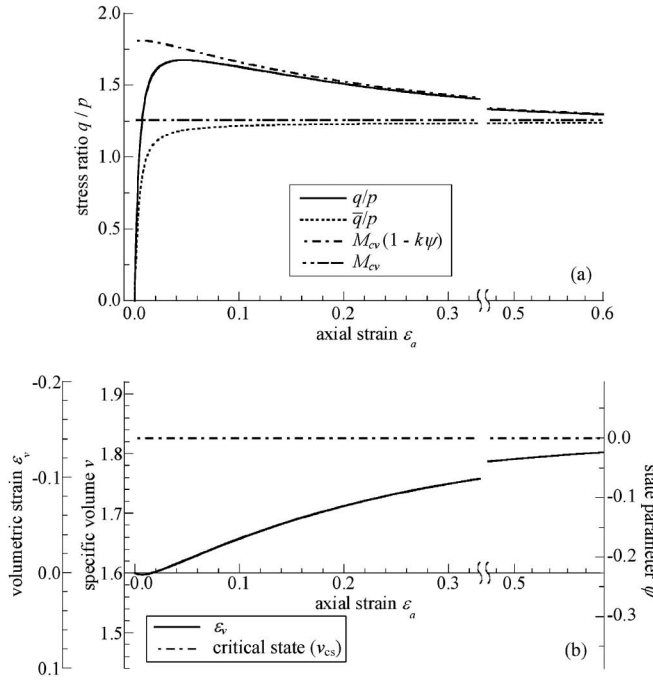


Fig. 20. An example of the simulation of drained triaxial compression test along a constant p' ($=100$ kPa) path (proposed model; dense sample $v_0 = 1.60$) (a) variations of stress ratio, normalised stress ratio and available strength against axial strain; (b) volumetric behaviour and variation of state parameter

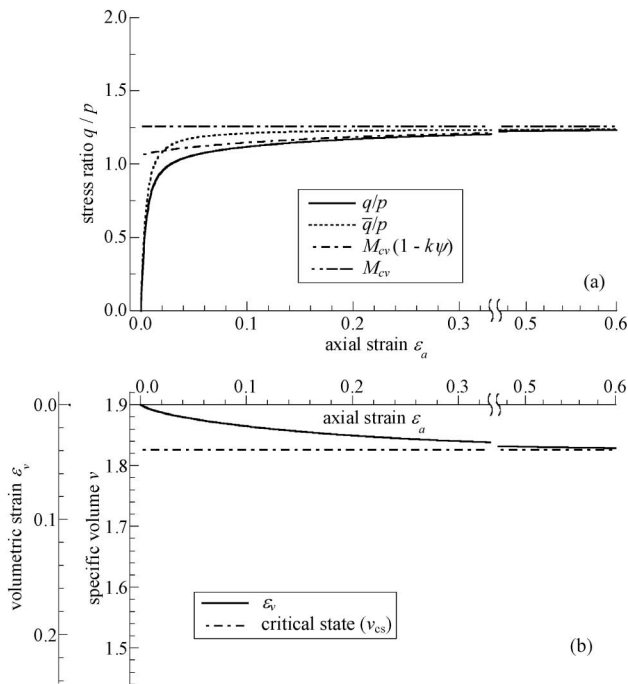


Fig. 21. An example of the simulation of drained triaxial compression test along a constant p' ($=100$ kPa) path (proposed model; loose sample $v_0 = 1.90$) (a) variations of stress ratio, normalised stress ratio and available strength against axial strain; (b) volumetric behaviour and variation of state parameter

strength $M_{cv}(1 - k\psi)$ are plotted against axial strain in Figs. 20(a) and 21(a), where M_{cv} ($=\eta_{cs}$) represents the critical state strength calculated from the critical state friction angle ϕ_{cv} . The corresponding volumetric behaviours are shown in Figs. 20(b) and 21(b). The strength of soil is generally dependent on density and confining pressure, and this characteristic is modelled by the variation in the available strength owing to the state parameter: the available strength is initially larger than the critical state strength for dense sand. This is because $\psi < 0$ and increases very slightly during the initial shearing with volumetric compression and asymptotically decreases again towards the critical state strength with positive dilatancy. While the available strength is smaller than the critical state strength for loose sand and increases monotonically towards the critical state strength owing to the volumetric compression. Meanwhile, the typical stress:strain relationship of sands with different initial densities are properly described: the stress ratio for loose sand monotonically increases to the critical state friction angle; the stress ratio for dense sand increases in the beginning stage of shearing, reaches a peak strength and asymptotically decreases towards the falling available strength. Such stress:strain behaviour including strain softening is described by a simple monotonic hardening law in the normalised stress space because the available strength is always fixed constant in the normalised stress space and the normalised stress asymptotically reaches towards it. The variations in the state parameter for dense and loose samples during drained shearing are plotted against axial strain in Figs. 20(b) and 21(b). Though the initial value of the state parameter ψ is negative for dense sand and vice versa, the state parameter asymptotically approaches zero due to shearing, by which variations in the available strengths for dense and loose samples are suitably described.

Second, a series of drained triaxial compression tests under different mean effective stresses p' , obtained by the original Severn-Trent sand and the proposed model, are compared. Figure 22 shows the stress paths imposed in the plane of mean effective stress p' and deviator stress q . Sample OE was sheared at constant mean effective stress from O to E without any variation in mean effective stress; sample OAF was compressed from O to A and sheared at constant mean effective stress; samples OBG, OCH and ODI were correspondingly compressed from O to B, C and D, respectively and sheared. Figures 23(a) and (b) show the relationships between the specific volume and the mean effective stress in the compression plane, obtained by the original Severn-Trent sand and the proposed model, respectively. In the simulations by the original model, volumetric compression during isotropic stress increase is slight and purely elastic, and specific volume tends to a unique critical state line (at which $I_G = 0$) due to shearing (Fig. 23(a)). On the other hand, the results obtained by the proposed model (Fig. 23(b)) are quite different from those obtained by the original model because the grading index I_G is increased by isotropic compression or shearing (Fig. 24). The critical state line

nal Severn-Trent sand. Variations in the stress ratio q/p' , the normalised stress ratio \bar{q}/p' and the current available

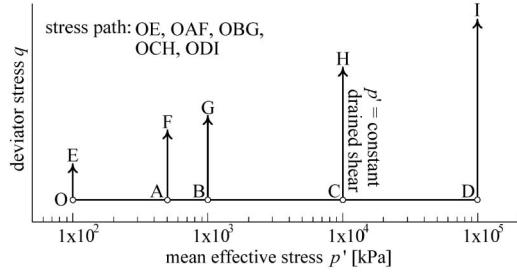


Fig. 22. Effective stress paths for the simulations of drained triaxial compression tests with different mean effective stress (paths OE, OAF, OBG, OCH, ODI)

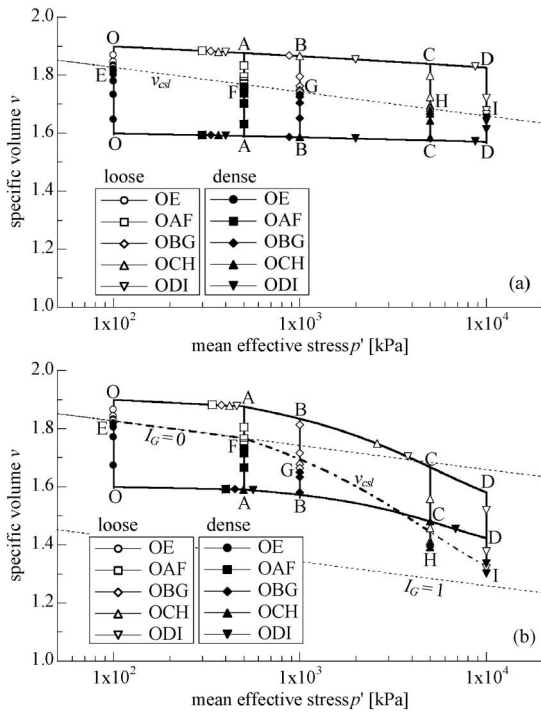


Fig. 23. Relationships between mean effective stress and specific volume for the simulations of isotropic compression and drained triaxial compression tests with different mean effective stress (a) original Severn-Trent sand model; (b) proposed model considering the effect of particle crushing

and isotropic compression line are lowered in the compression $v:\ln p'$ plane by the increase in the grading state index (Figs. 23(b) and 24). Typical stress:strain relationships for loose and dense samples along paths OE, OAF and OCH, obtained by the original Severn-Trent sand and the proposed model, are compared in Figs. 25, 26 and 27 respectively. The stress path OE is assumed to be a shearing path within the crushing surface, so that the grading state index I_G remains zero and the stress:strain responses by both models are identical (Fig. 25). In the simulations on the sample OAF, likewise the grading state index remains constant along the isotropic compression path from O to A. The stress state, however, reaches the initial position of the crushing surface at the stress point A, and the crushing surface is enlarged along the shearing path AF. Although the initial shear stiffness ob-

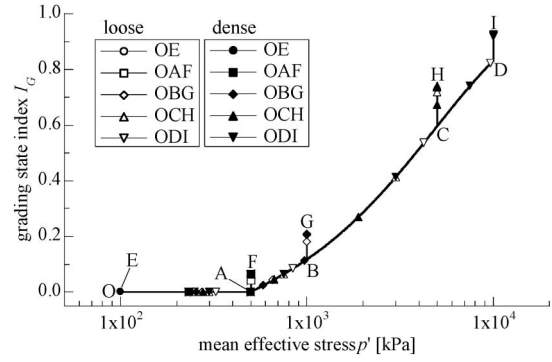


Fig. 24. Variations of the grading state index I_G for the simulation of drained triaxial compression tests with different mean effective stress, obtained by the proposed model (paths OE, OAF, OBG, OCH, ODI)

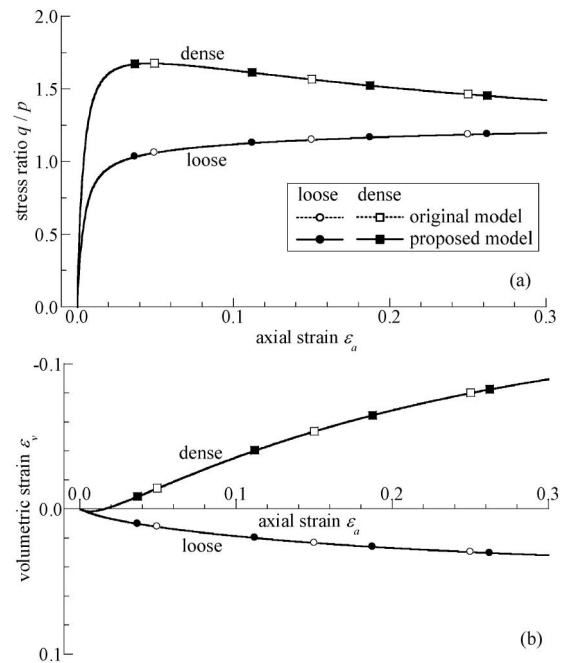


Fig. 25. Simulations of drained triaxial compression tests along a constant mean effective stress path (path OE)

tained by both models are same for each density, the grading state index is increased, critical state line is lowered, the state parameter is increased, soil feels looser and peak strength and dilatancy are slightly decreased (Fig. 26). Meanwhile, the grading state index is increased and the critical state line is lowered in the compression plane along isotropic compression paths OB, OC and OD, which makes the following shear behaviours quite different from those of the uncrushed samples (or simulations by the original Severn-Trent sand) (Fig. 27). It is known that the proposed model can describe the typical behaviour of crushable soils and that stress:strain behaviours of crushable soils are similar to those for looser soils of a less crushable nature. It is also indicated from Fig. 27 that typical influences of the particle crushing observed in the past experiments (Miura and O-Hara, 1979; Kato et

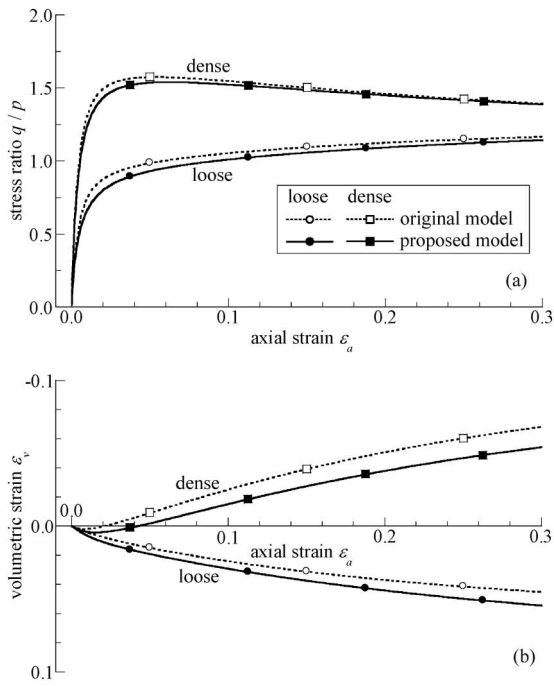


Fig. 26. Simulations of drained triaxial compression tests along a constant mean effective stress path (path OAF)

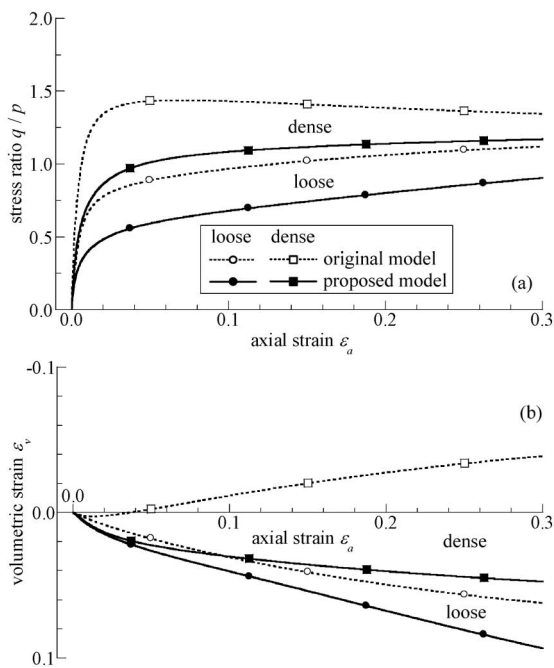


Fig. 27. Simulations of drained triaxial compression tests along a constant mean effective stress path (path OCH)

al., 2005) such as increase in negative dilatancy and decrease in peak shear strength are well described by the proposed model.

Third, a series of drained triaxial compression tests with constant mean effective stress p' have been performed with varying amounts of initial isotropic precompression to produce different changes in the grading index I_G . Figure 28 shows the effective stress path, while Fig. 29

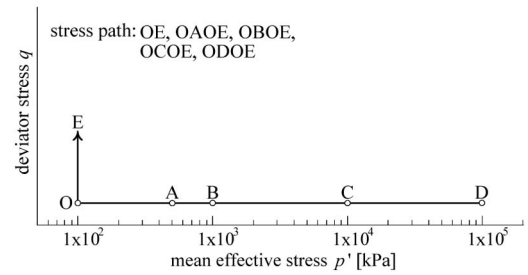


Fig. 28. Effective stress paths for the simulations of drained triaxial compression tests with different precompression histories (paths OE, OAOE, OBOE, OCOE, ODOE)

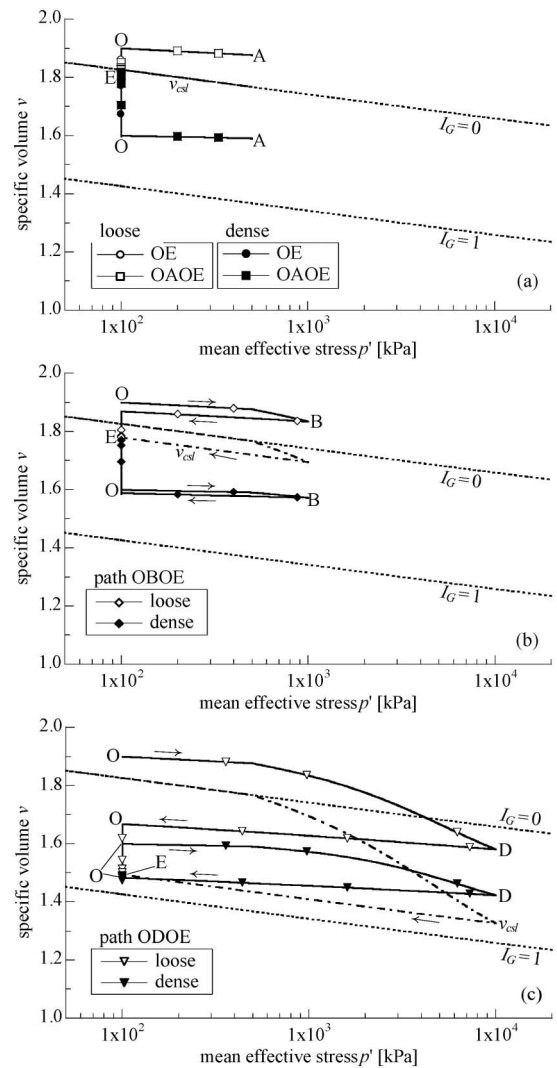


Fig. 29. Simulations of drained triaxial compression tests with precompression histories (a) stress paths OE, OAOE; (b) stress path OBOE; (c) stress path ODOE

shows the histories imposed in the plane of $\ln p':v$. Sample OE was sheared at constant mean stress from O to E without any precompression; sample OAOE was precompressed from O to A and back again and then sheared to E under constant mean effective stress—this is assumed to be a precompression excursion within the current crush-

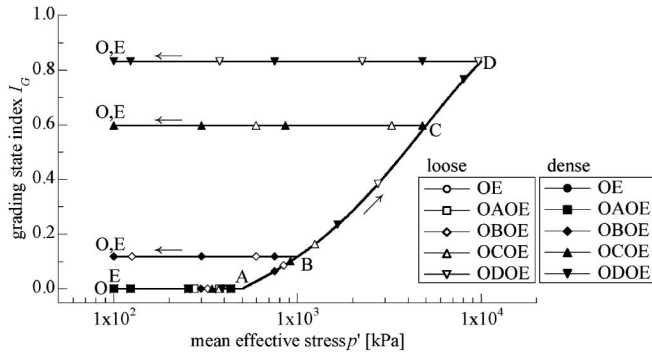


Fig. 30. Variations of the grading state index I_G for the simulation of drained triaxial compression tests with different precompression histories (stress paths OE, OAOE, OBOE, OCOE, ODOE)

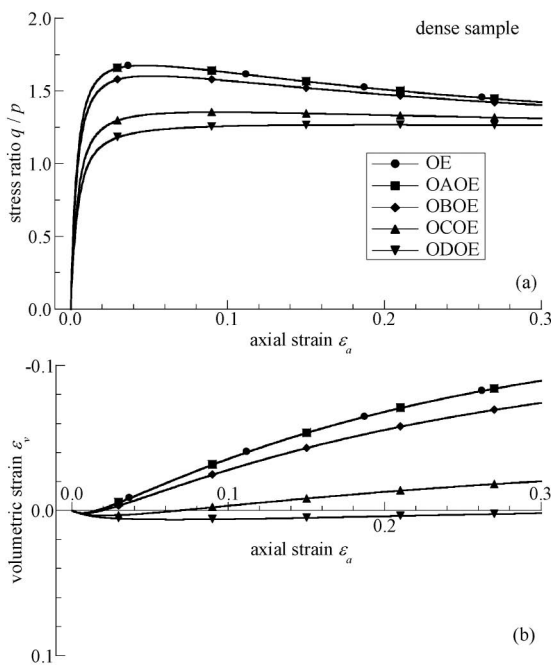


Fig. 31. Simulations of drained triaxial compression tests along a constant mean effective stress path with different precompression histories (dense samples): (a) stress:strain response; (b) volumetric response

ing surface; samples OBOE, OCOE and ODOE were correspondingly pre-compressed from O to B, C and D respectively and back again to O and then sheared—for these samples crushing occurs and the grading state index increases during precompression process (Fig. 30) (Point E denotes a failure state which will be different for each sample.). The effect of the precompression is to crush some of the particles and hence to increase I_G and hence to lower the critical state line. The value of state parameter just before shearing at O increases as the extent of the precompression increases and the subsequent stress:strain:dilatancy responses change gradually from those expected of a dense material to those expected of a loose material (Figs. 31 and 32): the peak strength decreases from the stress:strain response and the amount of volumetric expansion accompanying shear reduces

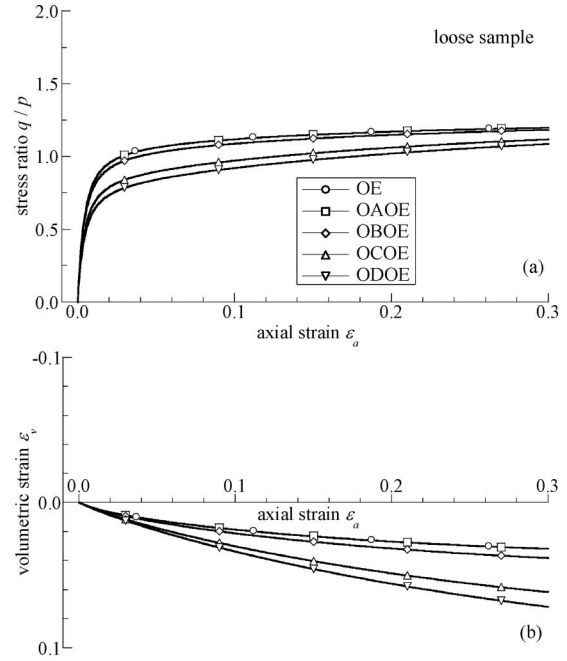


Fig. 32. Simulations of drained triaxial compression tests along a constant mean effective stress path with different precompression histories (loose samples): (a) stress:strain response; (b) volumetric response

with increasing the amount of precompression. Without particle crushing the response of all four samples would be identical to that of sample OE.

Simulations of Undrained Triaxial Compression Tests

A series of undrained triaxial compression tests, for which the initial value of mean effective stress is same, have been performed on samples with different initial densities. The paths in the compression plane and the effective stress paths, obtained by the original model and the proposed model, are compared in Figs. 33 and 34, respectively. For loose samples (with initially positive values of state parameter) undrained constant volume shearing has to end up on the critical state line at a low stress level. Such a test hardly engages with the crushing criterion so that the results by the proposed model are identical to those by the original model and the effect of including particle crushing is negligible. On the other hand tests on initially dense samples (with initially negative values of state parameter) show typically some contractive initial behaviour, with the mean effective stress falling, followed by some volumetric dilation which translates into mean effective stress increase in these samples. Increase in mean effective stress in the sample with initial specific volume of 1.8 is within the current crushing surface and the grading state index remains zero. However, for the simulations shown in which the initial specific volume is less than 1.7, the effective mean stress increases, some particle crushing occurs, the grading state index increases (Fig. 35), and the critical state line falls (Fig. 33(b)). The importance of the downward evolution of the critical state line is obvious: without this down-

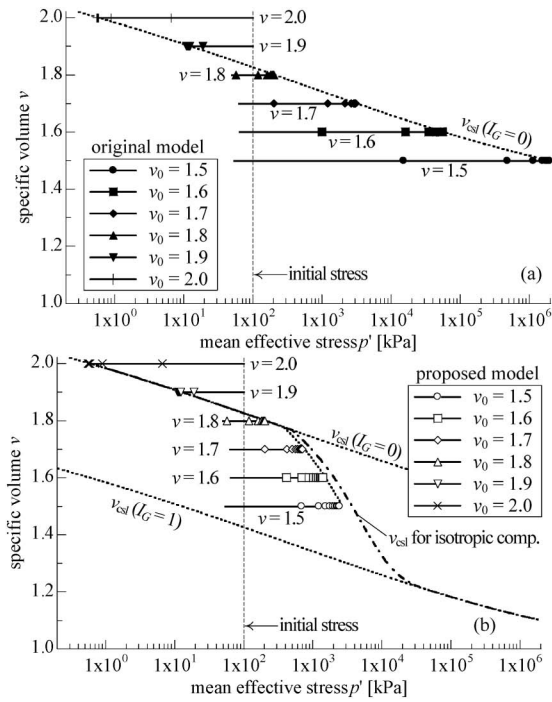


Fig. 33. Relationships between mean effective stress and specific volume for the simulations of undrained triaxial compression tests with different initial densities: (a) original Severn-Trent sand model; (b) proposed model considering the effect of particle crushing

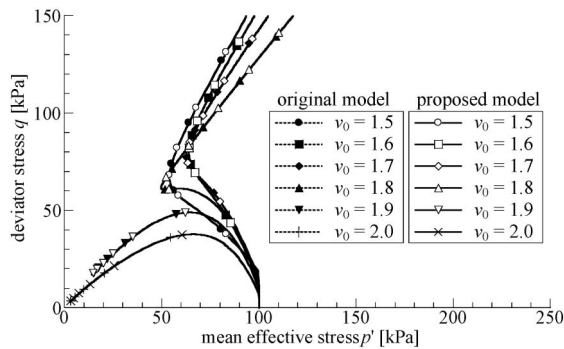


Fig. 34. Effective stress paths for the simulations of undrained triaxial compression tests with different initial densities

turn the effective stress paths of the denser samples would in principle meet the unchanging critical state line at extremely high effective stresses (Fig. 33) though the effective stress paths obtained by both models are identical in relatively small stress level (Fig. 34); strain softening after the peak shear strength in stress:strain responses becomes calm due to the effect of particle crushing (Fig. 36).

CONCLUSIONS

A model has been developed which incorporates necessary descriptions of aspects of constitutive behaviour of granular materials. In particular these include (a) a critical state line which exists for all possible specific volumes

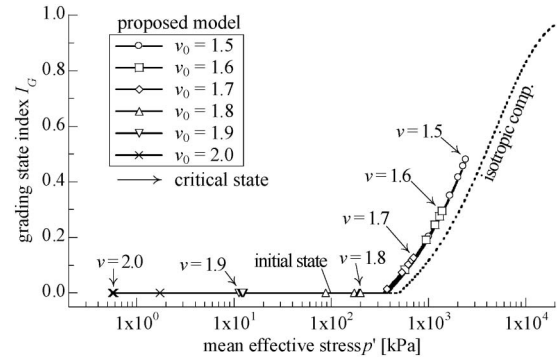


Fig. 35. Variations of the grading state index I_G for the simulation of undrained triaxial compression tests with different initial densities (proposed model)

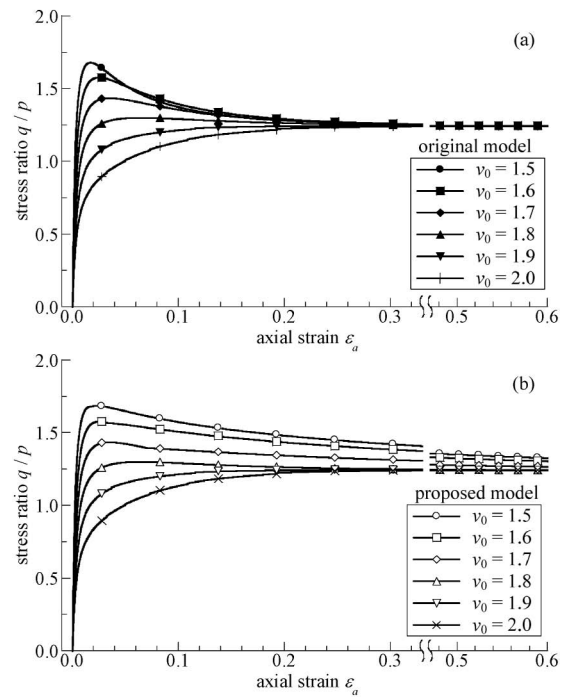


Fig. 36. Stress:strain responses for the simulations of undrained triaxial compression tests with different initial densities: (a) original Severn-Trent sand model; (b) proposed model considering the effect of particle crushing

that are present in the soil samples; (b) a dependency of current strength on current value of state parameter which in general changes as the soil dilates as it is sheared; (c) the evolution of limiting states with changing particle sized distribution due to particle crushing described through a grading state index. The effect of crushing is to shift the critical state line and compression line downwards in the compression plane because broader gradings are able to pack more efficiently. As a consequence the crushing soil feels looser and dense samples as they crush show aspects of drained and undrained behaviour which are more reminiscent of loose materials.

Finally, it is stated that the proposed concept of the three dimensional critical state surface in the space of mean effective stress, specific volume and grading state

index (or the idea of shifting position of the critical state line in the compression plane due to changing grading) can be applied to other phenomena involving variation in the particle size distribution such as: (a) loss of fines (internal erosion); (b) phase transition of solid and void fluid; (c) physical weathering due to the variation in stresses, temperature and hygroscopic behaviour; and (d) chemical weathering. The extension of the evolution law for the grading state index I_G considering each phenomenon is, however, an issue for future study.

ACKNOWLEDGEMENTS

This research would not have been possible without the generous support of the Japan Society for the Promotion of Science (JSPS) enabling collaboration visits of Mamoru Kikumoto to Bristol and David Muir Wood to Nagoya. This work is also supported by JSPS Grant-in-Aid for Young Scientists (20860045) provided to Mamoru Kikumoto. The financial support provided to Adrian Russell through an UNSW Early Career Researcher Grant for his visit to Nagoya and for Mamoru Kikumoto to visit Sydney is also gratefully acknowledged.

REFERENCES

- Alawaji, H., Alawi, M., Ko, H.-Y., Sture, S., Peters, J. F. and Muir Wood, D. (1990): Experimental observations of anisotropy in some stress-controlled tests on dry sand, *Yielding Damage, and Failure of Anisotropic Solids* (ed. by Bohler, J. P.) Mechanical Engineering Publications, London, EGF5, 251–264.
- Been, K. and Jefferies, M. G. (1985): A state parameter for sands, *Géotechnique*, **35**(2), 99–112.
- Bopp, P. A. and Lade, P. V. (2005): Relative density effects on undrained sand behavior at high pressures, *Soils and Foundations*, **45**(1), 15–26.
- Cheng, Y. P., Bolton, M. D. and Nakata, Y. (2005): Grain crushing and critical states observed in DEM simulations, *Powders and Grains* (eds. by García-Rojo, Herrmann and McNamara), Taylor and Francis Group, London, **2**, 1393–1397.
- Coop, M. R. (1990): The mechanics of uncemented carbonate sands, *Géotechnique*, **40**(4), 607–626.
- Coop, M. R. and Lee, I. K. (1993): The behaviour of granular soils at elevated stresses, *Predictive Soil Mechanics, Proc. C. P. Wroth Memorial Symposium*, Thomas Telford, London, 186–198.
- Coop, M. R., Sorensen, K. K., Bodas Freitas, K. K. and Georgoutsos, G. (2004): Particle breakage during shearing of a carbonate sand, *Géotechnique*, **54**(3), 157–163.
- Dafalias, Y. F. (1986): Bounding surface plasticity. I: Mathematical foundation and hypoplasticity, *J. Eng. Mech.*, ASCE, **112**(9), 966–987.
- Gajo, A. and Muir Wood, D. (1999a): A kinematic hardening constitutive model for sands: the multiaxial formulation, *Int. J. Numer. Anal. Methods Geomech.*, **23**(5), 925–965.
- Gajo, A. and Muir Wood, D. (1999b): Severn-Trent sand: a kinematic hardening constitutive model for sands: the q - p formulation, *Géotechnique*, **49**(5), 595–614.
- Gudehus, G. (1997): Attractors, percolation thresholds and phase limits of granular soils, *Powders and Grains '97* (eds. by Behringer, R. P. and Jenkins, J. T.), Rotterdam, Balkema, 169–183.
- Hales, T. C. (2005): A proof of the Kepler conjecture, *Annals of Mathematics*, **162**, 1065–1185.
- Hardin, B. O. (1985): Crushing of soil particles, *J. of Geotech. Eng.*, ASCE, **111**(10), 1177–1192.
- Hashiguchi, K. (1980): Constitutive equation of elastoplastic materials with elasto-plastic transition, *J. of Appl. Mech.*, ASCE, **102**(2), 266–272.
- Hyodo, M., Hyde, A. F. L. and Aramaki, N. (1998): Liquefaction of crushable soils, *Soils and Foundations*, **48**(4), 527–543.
- Hyodo, M., Hyde, A. F. L., Aramaki, N. and Nakata, Y. (2002): Undrained monotonic and cyclic shear behaviour of sand under low and high confining stresses, *Soils and Foundations*, **42**(3), 63–76.
- Kasner, E. and Supnick, F. (1943): The apollonian packing of circles, *Natl. Acad. Sci.*, **29**, 378–384.
- Kato, S., Nonami, S. and Sakakibara, T. (2005): Effect of particle crushability on critical state line of granular material, *Powders and Grains 2005* (eds. by García-Rojo, Herrmann and McNamara), AA Balkema Publishers, Leiden, **2**, 1399–1403.
- Koiter, W. T. (1953): Stress-strain relations, uniqueness and variational theorems for elastic-plastic materials with a singular yield surface, *Quart. Appl. Math.*, **11**, 350–354.
- Lade, P. V., Liggio, Jr., C. D. and Yamamuro, J. A. (1998): Effects of non-plastic fines on minimum and maximum void ratios of sand, *Geotech. Testing J.*, **21**(4), 336–347.
- Mahboubi, A., Cambou, B. and Fry, J. J. (1997): Numerical modelling of the mechanical behaviour of non-spherical crushable particles, *Powders and Grains '97* (eds. by Behringer, R. P. and Jenkins, J. T.), Rotterdam, Balkema, 139–142.
- McDowell, G. R., Bolton, M. D. and Robertson, D. (1996): The fractal crushing of granular materials, *J. Mech. Phys. Solids*, **44**(12), 2079–2102.
- Miura, N. and O-Hara, S. (1979): Particle-crushing of a decomposed granite soil under shear stresses, *Soils and Foundations*, **19**(3), 2–14.
- Muir Wood, D. (1990): *Soil Behaviour and Critical State Soil Mechanics*, Cambridge University Press.
- Muir Wood, D. (2007): The magic of sands: 20th Bjerrum Lecture presented in Oslo 25 November 2005, *Can. Geotech. J.*, **44**(11), 1329–1350.
- Muir Wood, D. and Maeda, K. (2007): Changing grading of soil: effect on critical states, *Acta Geotechnica*, **3**(1), 3–14.
- Nakai, T. (1989): An isotropic hardening elastoplastic model for sand considering the stress path dependency in three-dimensional stresses, *Soils and Foundations*, **29**(1), 119–137.
- Roberts, J. E. and de Souza, J. M. (1958): The compressibility of sands, *Proc. of the American Society for Testing and Materials*, **58**, 1269–1277.
- Russell, A. R. and Khalili, N. (2002): Drained cavity expansion in sands exhibiting particle crushing, *Int. J. Numer. Anal. Methods Geomech.*, **26**(4), 323–340.
- Russell, A. R. and Khalili, N. (2004): A bounding surface plasticity model for sands exhibiting particle crushing. *Can. Geotech. J.*, **41**, 1179–1192.
- Russell, A. R., Muir Wood, D. and Kikumoto, M. (2009): Crushing of particles in idealized granular assemblies, *J. Mech. Phys. Solids*, **57**(8), 1293–1313.
- Schofield, A. N. and Wroth, C. P. (1968): *Critical State Soil Mechanics*, McGraw-Hill, London.
- Tojo, A., Yamada, S. and Sato, K. (2009): Experimental study on the influence of particle crushing on the critical states of sandy soils, *Proc. Annual Conf. of Japanese Society for Civil Engineers Seibu Branch*, CD-ROM (in Japanese).
- Vesić, A. S. and Clough, G. W. (1968): Behavior of granular materials under high stresses, *J. Soil Mech. Found. Div.*, **94** SM3, 661–688.
- Zlatović, S. and Ishihara, K. (1995): On the influence of nonplastic fines on residual strength, *Earthquake Geotech. Eng.* (ed. by Ishihara), 239–244.